

## The Fractal Nature of Drought: Power Laws and Fractal Complexity of Arizona Drought

Sepideh Azizi<sup>1</sup>, Tahmineh Azizi<sup>2,\*</sup>

<sup>1</sup>*Department of Urban Planning and Design, Shiraz University, Iran  
sepid.azizi97@gmail.com*

<sup>2</sup>*Department of Mechanical Engineering, Florida State University, USA  
tazizi@fsu.edu*

\*Correspondence: [tazizi@fsu.edu](mailto:tazizi@fsu.edu)

**ABSTRACT.** In this study, we explore the possibility that the Drought Monitor database belongs to class of fractal process which can be characterized using a single scaling exponent. The Drought Monitor map identifies areas of drought and labels them by intensity:  $D_0$  abnormally dry,  $D_1$  moderate drought,  $D_2$  severe drought,  $D_3$  extreme drought, and  $D_4$  exceptional drought. The vibration analysis using power spectral densities (PSD) method has been carried out to discover whether some type of power-law scaling exists for various statistical moments at different scales of this database. We perform multi-fractal analysis to estimate the multi-fractal spectrum of each group. We apply Higuchi algorithm to find the fractal complexity of each group and then compare them for different time intervals. Our findings reveal that we have a wide range of exponents for  $D_0$ - $D_4$ . Therefore,  $D_0$ - $D_4$  belong to class of multi-fractal process for which a large number of scaling exponents are required to characterize the scaling structure.

### 1. INTRODUCTION

Drought is defined as a moisture deficit bad enough to have social, environmental or economic effects. Drought is a recurring feature of nearly every climate on the planet [1–5]. In many parts of the world, including North America, we have little ability to predict exactly when drought will happen next. But if we look at history and climate data, we can be sure that drought will happen again at some point. In the United States, a well-developed economy and agricultural system generally protect citizens from the most critical effects of drought such as shortages of food and water. However, drought still causes extreme hardship for farm and ranch families, and individual wells may run dry. Besides affecting municipal water suppliers, drought affects businesses and environmental interests that are reliant on adequate and timely amounts of precipitation and water, such as habitat for fish and wildlife, outdoor recreation outfitters, and landscaping and car

---

Received: 2 Mar 2022.

*Key words and phrases.* fractional geometry; power spectral densities (PSD); multifractal analysis; fractal dimension; drought.

wash services [5–14]. The Drought Monitor map identifies areas of drought and labels them by intensity.  $D_1$  is the least intense level and  $D_4$  the most intense.  $D_0$  areas are not in drought, but are experiencing abnormally dry conditions that could turn into drought or are recovering from drought but are not yet back to normal.

There are different indices which have been used to assess drought severity and impacts in different time-scales. The normalized difference vegetation index (NDVI) is one of the most widely utilized drought indices to determine different drought levels [15–17]. Satellite databases have been extensively used to record and quantify the changes that may happen in vegetation coverage due to changing climate conditions. The NDVI is estimated using visible and near-infrared (NIR) bands from Advanced Very-High-Resolution Radiometer (AVHRR), Terra Moderate Resolution Imaging Spectroradiometer (MODIS), and Landsat sensors. In general, positive NDVI values demonstrate vegetated areas, zero and negative values are associated with bare soil and water bodies [15]. The time series of the average NDVI for Arizona (Arizona includes regions with moderate to exceptional drought  $D_1$ – $D_4$ ) shows the highest and lowest NDVI values during 10 years (2010–2020) (for the month of Jan–Dec each year) (see figure (1)). The NDVI data selected from the Google Earth Enterprise open source which is derived using Terra Moderate Resolution Imaging Spectroradiometer (MODIS) and would be useful to forecast the future changes in vegetation in Arizona. Each state experiences different set of impacts during a drought. We have also displayed the table of reported impacts during past droughts in Arizona for each level of drought on the U.S. Drought Monitor in table (2) (Source(s): NDMC, NOAA, USDA). When we study real world time series data, depending on scale and higher order moments, we may confront with data that display nonlinear power-law behaviours. For these type data, we need to apply multifractal analysis. In multifractal analysis we discover whether some type of power-law scaling exists for various statistical moments at different scales. A process called mono-fractal, if it can be characterized using a single scaling exponent, or this process is a linear function of the moments. Likewise, a process called multi-fractal, if we see the scaling behavior follows a function which is non-linear in the moments. When we study scale invariant time series data, or data with different scaling behavior, we are not able to use the classical time series analysis and we need to perform fractal analysis.

In this study, we use fractal geometry to classify drought severity from 2000 to 2021 in Arizona. We perform multifractal analysis to discover whether some type of power-law scaling exists for various statistical moments at different scales of these data sets. We plot the multifractal spectra to compare the width of the scaling exponent for each spectrum. A quantitative analysis commonly known as the Fractal Dimension (FD) using Higuchi algorithm.

## 2. MATERIALS, METHODS AND RESULTS

**2.1. Data.** Here, data has been collected using U.S. Drought Monitor for each week of the selected time period (January 2000 to Nov 2021) and location (Arizona, USA), see figures (3) and (4). The

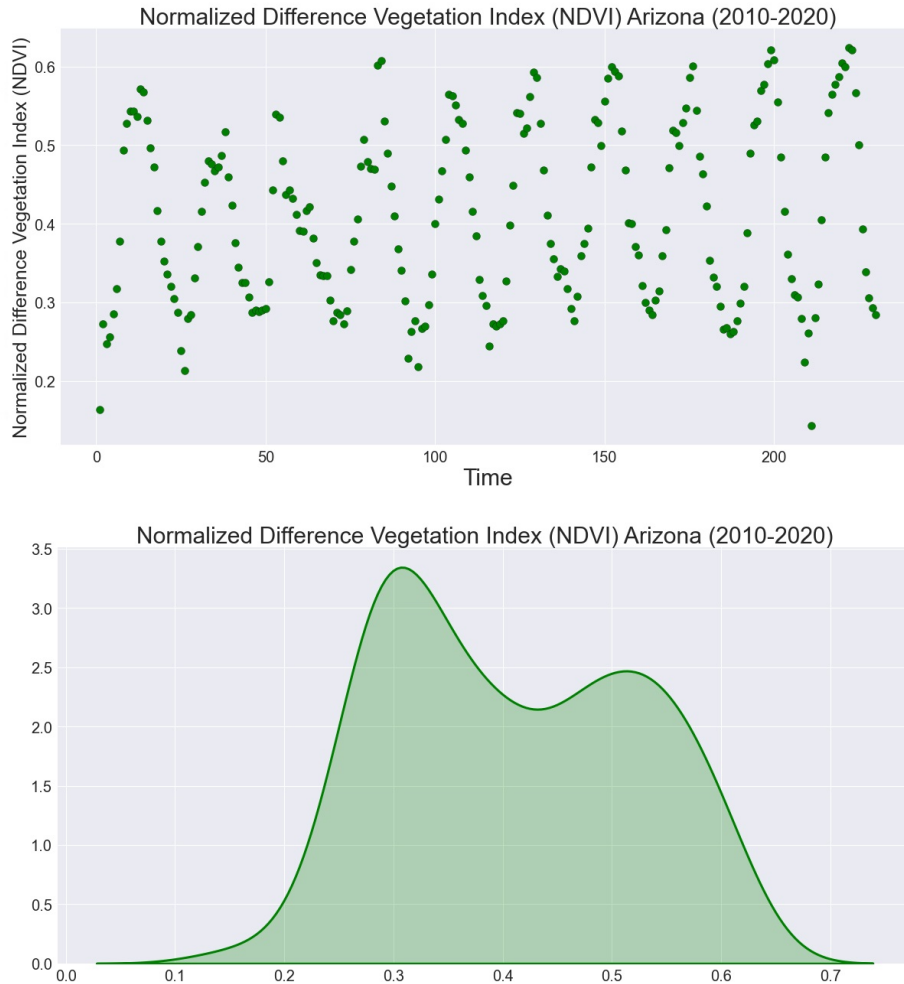


FIGURE 1. Normalized Difference Vegetation Index (NDVI) Arizona between 2010-2020; Google Earth Enterprise Open Source

U.S. Drought Monitor which started from 1999, is a partnership between the National Drought Mitigation Center (NDMC) at the University of Nebraska-Lincoln, the United States Department of Agriculture (USDA), and the National Oceanic and Atmospheric Administration (NOAA). Each Thursday, the U.S. Drought Monitor (USDM) will be updated to demonstrate the location and intensity of drought across the country. Using the experts' assessments, drought categories display conditions related to dryness and drought such as observations of how much water is available in streams, lakes, and soils compared to usual time of year (Source(s): NDMC, NOAA, USDA) [18].

**2.2. Time-Frequency Analysis and Continuous Wavelet Transform (CWT).** Continuous Wavelet Transform (CWT) provides a linear time-frequency representation of non-stationary signals called scalogram by breaking the data into scales by preserving time shifts and time scales. Therefore, the wavelet transform makes the analysis of the data in different frequency ranges easier and we can

Category	Historically observed impacts
D0	Forage crops and pasture are stressed; producers feed livestock early
	Ground is hard
	Agriculture ponds and creeks begin to decline
D1	Cash crop growth and yield are low
	National forests implement campfire and firework bans
	Streams and ponds are low
	Fire activity increases
D2	Crops are damaged, especially dryland corn
	Burn bans begin
	Large cracks appear in foundations of homes
	Large surface water levels drop; agricultural ponds and streams have dried up
	Saltwater intrusion occurs in rivers and bays; saltwater wildlife migrate upstream
	Hydroelectric power decreases; navigation is limited
D3	Soybean pods shatter
	Large-scale hay shortages occur; producers sell livestock
	Wildfire count and fire danger continue to increase
	Landscape growth is stunted and needs irrigation; Christmas tree growth is stunted
	Ground has noticeable cracks; road damage has occurred
	Low flow in rivers and lakes affects recreation
	Water mains break daily in large municipalities; water conservation is implemented
	Air quality is poor
D4	Trees and shrubs are defoliated; grass is brown; landscaping projects are delayed
	Wildfire count is very high
	Lakes are extremely low; large municipalities implement water restrictions; water prices increase

FIGURE 2. Table of the reported impacts during past droughts in Arizona for each level of drought on the U.S. Drought Monitor; (Source(s): NDMC, NOAA, USDA)

extract useful information from the time intervals between its consecutive waves of the data [19]. To compute the scalogram of data which is function of time and frequency, at first we split the time series data into overlapping segments, then we need to compute the absolute value of the continuous wavelet transform coefficients of each segment and finally, plot it. We have displayed the scalogram plots of Drought Monitor Categories Arizona database (2000 – present) in figures (5)-(6).

**2.3. Vibration frequency analysis using Power spectral densities (PSD).** The fast Fourier transform (FFT) has been used widely to analysis of vibration frequency in computing discrete Fourier transform (DFT). However, FFT only works accurately if we have a finite number of dominant frequency components. To overcome this problem, we use the power spectral densities (PSD) which

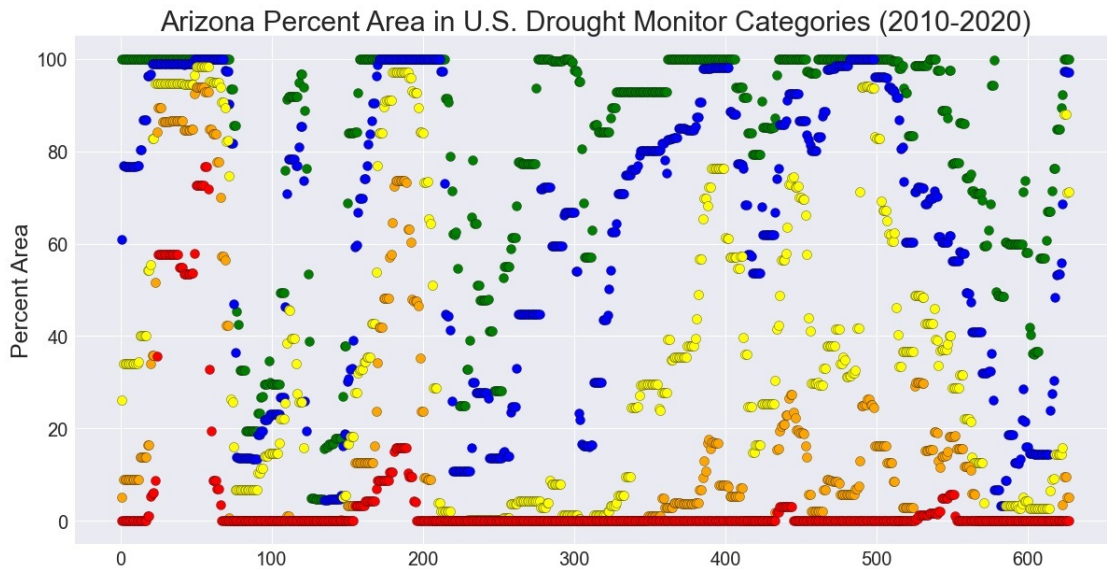


FIGURE 3. Arizona Percent Area in U.S. Drought Monitor Categories database (2000 - present); National Drought Mitigation Center (NDMC), the U.S. Department of Agriculture (USDA), and the National Oceanic and Atmospheric Administration (NOAA)

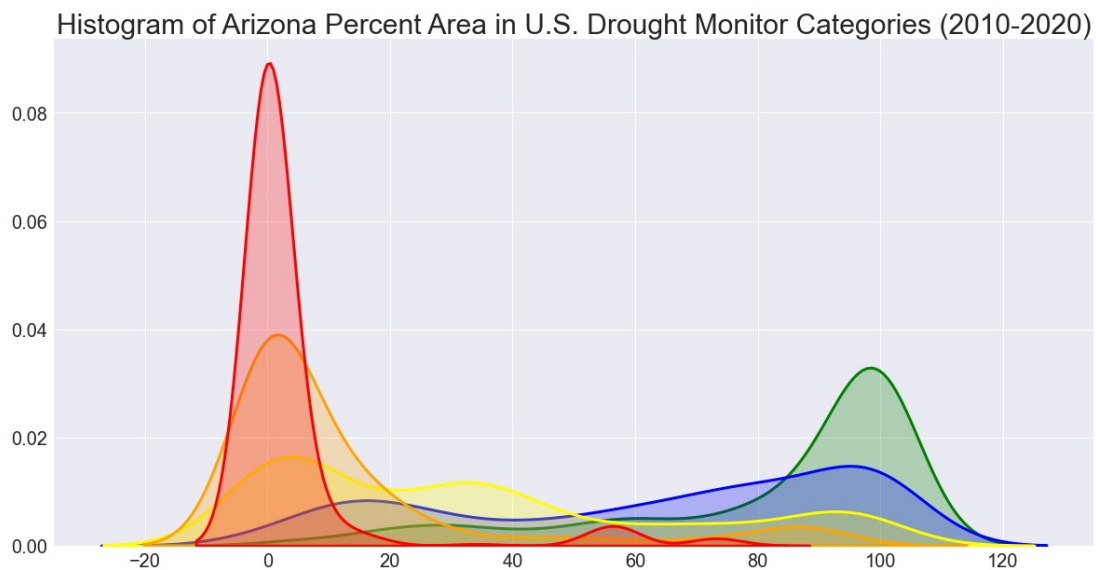


FIGURE 4. Histogram of Arizona Percent Area in U.S. Drought Monitor Categories database (2000 - present); National Drought Mitigation Center (NDMC), the U.S. Department of Agriculture (USDA), and the National Oceanic and Atmospheric Administration (NOAA)

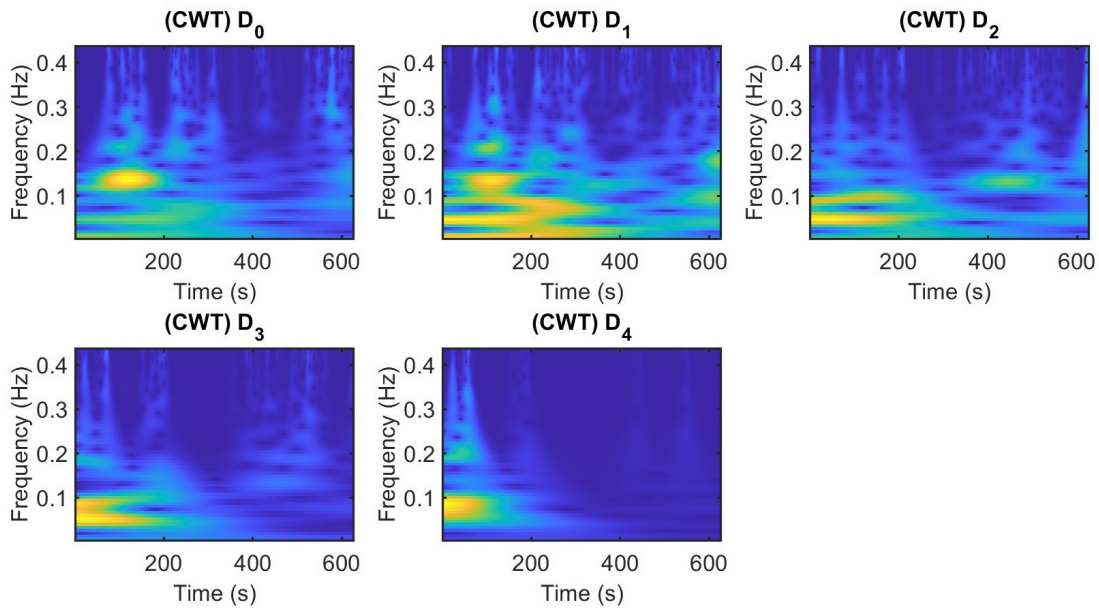


FIGURE 5. Time-frequency representations of Drought Monitor Categories database (2000 - present) using Continuous Wavelet Transform (CWT) in two dimensional Time-Frequency space

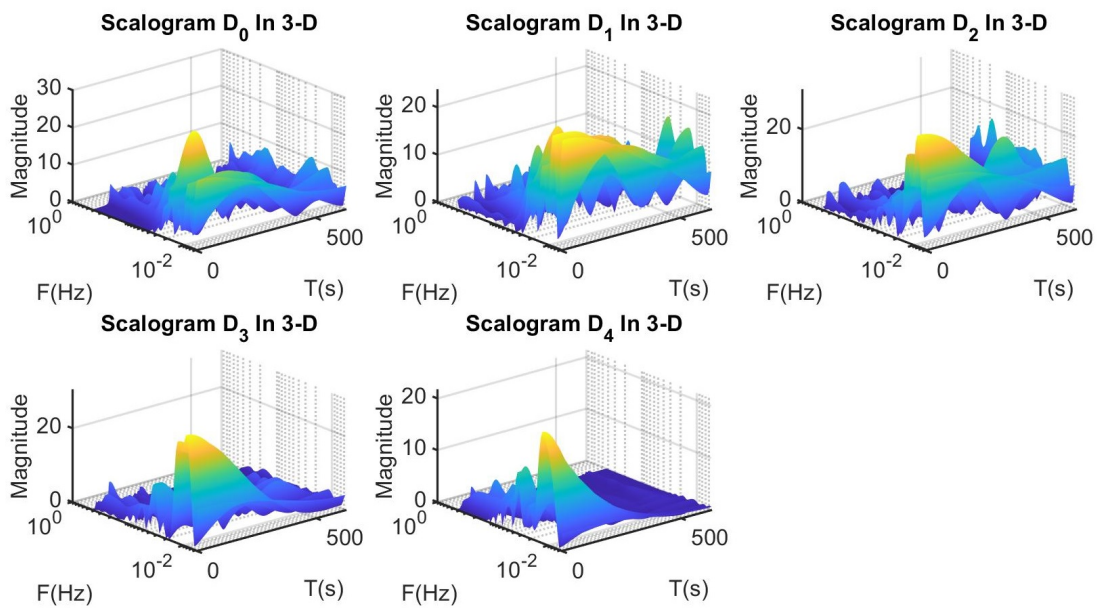


FIGURE 6. Time-frequency representations of Drought Monitor Categories database (2000 - present) using Continuous Wavelet Transform (CWT) in three dimensional Time-Frequency-Magnitude space

is applied to characterize random vibration in time series data. To compute PSD, we multiply each frequency bin of FFT by its complex conjugate to get a real spectrum and then normalize the results

to frequency bin width. Here, we have applied the (PSD) method for our database and then we fit the logarithm power spectral densities to their frequencies in log format using least squares approximation method. Finally, we calculate the slope for each regression line captures the linearity of data. In figure (7), we can see the fitted least squares approximation to the logarithm of power spectral density of Arizona drought database.

Moreover, we have plotted the scaling exponent graphs for Arizona drought database in figure (8).

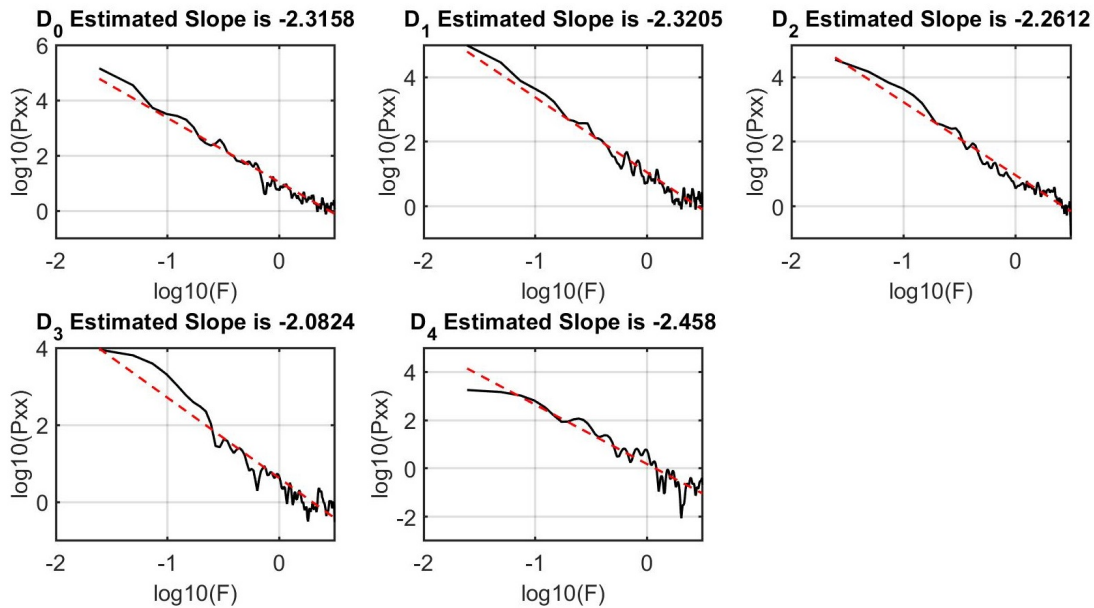


FIGURE 7. Fitted least squares approximation to the logarithm of power spectral density of Arizona drought database (2000 – present) obtained by wavelet techniques

**2.4. Multifractal Analysis and Discrete Wavelet Transform (DWT).** Fractal dimension is one of the most often used algorithm to describe the complexity of a fractal object by measuring the changes of coverings relative to the scaling factor [20–25]. It also specifies the space filling capacity of a fractal object with respect to its scaling properties in the space [26–29]. The relationship between scaling and covering is often hard to be characterized. The variation in the number of coverings,  $N(\epsilon)$ , with respect to the scaling factor  $\epsilon$ , can be written as

$$N(\epsilon) \propto \epsilon^{-D} \quad (1)$$

where  $D$  is the fractal dimension. The relation (1) is called scaling law that is used to demonstrate the size distribution of many objects in nature. The box counting formula which has been widely

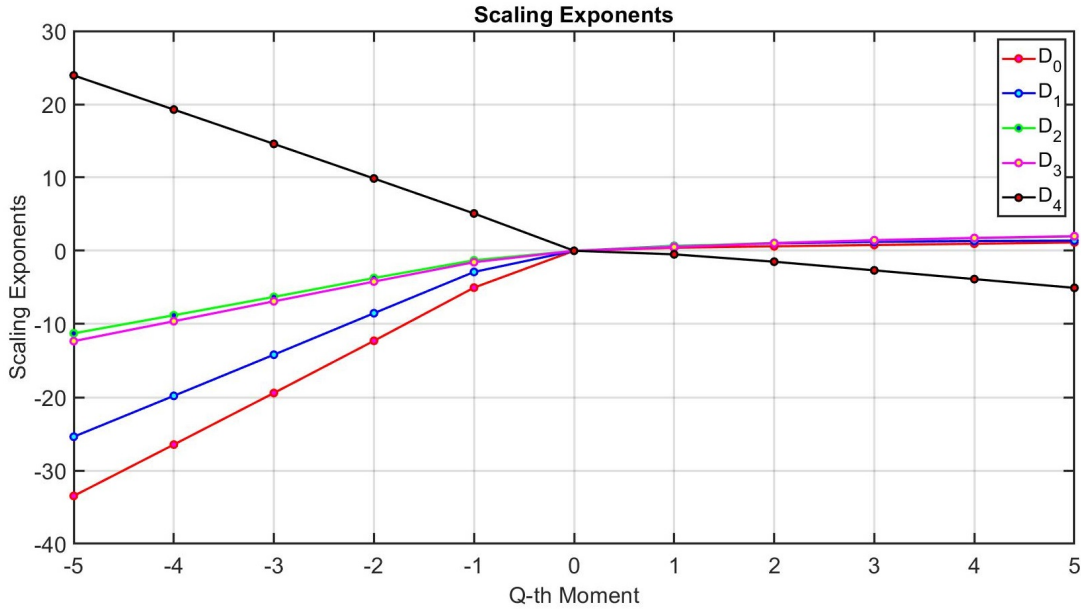


FIGURE 8. Scaling exponent of power spectral density for Drought Monitor Categories database (2000 - present).

applied to approximate the fractal dimension of an irregular object is defined as

$$D_B = \lim_{a \rightarrow 0} \frac{\ln(N(a))}{\ln(1/a)} \quad (2)$$

However, this monofractal dimension is not able to fully characterize complex scaling behaviors of many irregular objects in the real world. That's why to study irregular objects we need to apply the multifractal algorithm. The multifractal analysis utilizes a spectrum of singularity exponents to provide a detailed and local description of complex scaling behaviors. In order to quantify local densities of the fractal set, we approximate the mass probability using the following formula

$$P_i(a) = \frac{N_i(a)}{N} \quad (3)$$

where  $N_i(a)$  is the number of mass in the  $i$ th subset of measure  $a$ ,  $N$  is the total mass of the set. When we scale the mass probability  $P_i(a)$  with measure  $a$  of a multifractal set, it also demonstrates the power law behavior:

$$P_i(a) \propto a^{\alpha_i} \quad (4)$$

where  $\alpha_i$  is the singularity exponent characterizing the local scaling in the  $i$ th subset. The multifractal spectrum  $f(\alpha)$  provides a statistical distribution of singularity exponents  $\alpha_i$ . In general,

$f(\alpha)$  may be estimated using the Legendre transformation

$$f(\alpha) = q\alpha - \tau(q)$$

$$\alpha(q) = \frac{d\tau(q)}{dq}$$

where  $q$  is the moment and  $\tau(q)$  is the mass exponent of the  $q$ th order moment. In addition, the multifractal measures may be specified by scaling of  $q$ th moments of  $P_i(a)$  as

$$\sum_{i=1}^{N(a)} P_i^{q(a)} \propto a^{\tau(q)} = a^{(q-1)D_q} \quad (5)$$

where  $D_q = \frac{\tau(q)}{(q-1)}$  is the generalized fractal dimension. For  $q = 0$  equation (2.4) becomes

$$N(a) \propto a^{-D_0}$$

which is similar to formula (1).

From multifractal analysis results of Arizona drought database (see figure (9)), we can easily see that we have a wide range of exponents for  $D_0$ - $D_4$ , which indicates they have multifractal structure. The drought database needs to be indexed by different exponents as we decompose them into different subsets. Therefore,  $D_0$ - $D_4$  require much more exponents to characterize their scaling properties.

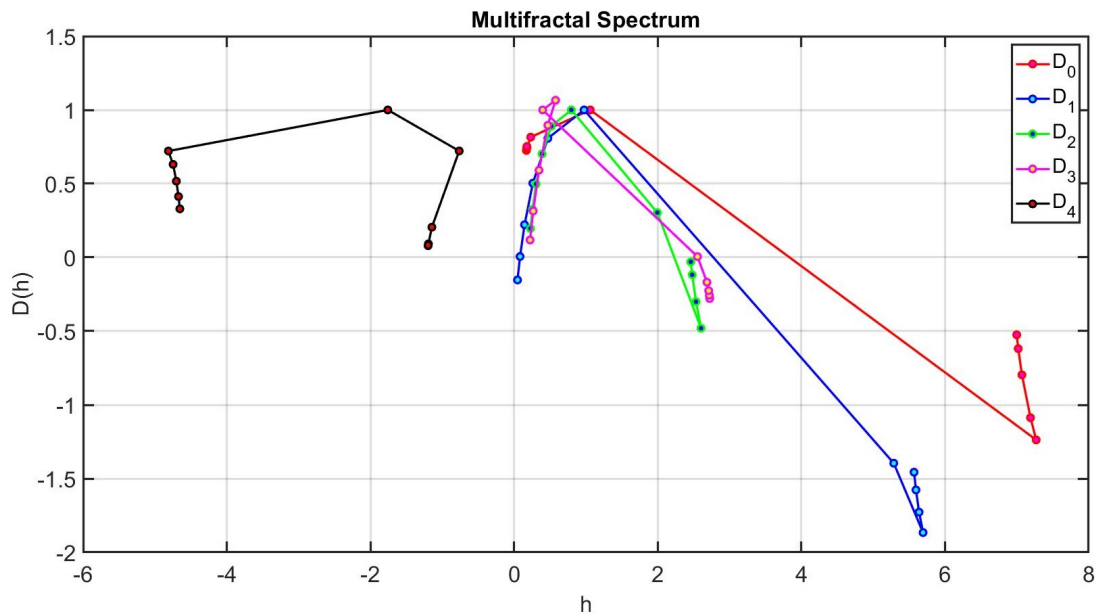


FIGURE 9. The multi-fractal spectrum analysis of Arizona Drought Monitor Categories database (2000 - present) shows the occurrence of multi-fractality with a broad range of exponents in data structure of  $D_0$ - $D_4$ .

**2.5. Higuchi Fractal Dimension Algorithm.** When we Use box counting method, we compute the fractal dimension and or the complexity of a fractal process in two dimensional space [30]. However, when we are working with many real world time series data, it fails to recognize the sudden changes happen in data [31]. To solve this problem, there are different methods such as Higuchi algorithm, power spectrum analysis, and Katz algorithm that help to analyze the complexity of irregular data [32–34]. Here we use Higuchi Algorithm. We start with a finite time series  $x_1, x_2, x_3, \dots, x_N$ . Then, we create  $k$  new time series  $x_m^k$  of the form

$$x_m, x_{m+k}, x_{m+2k}, \dots, x_{[m+Ak]}$$

where  $A = (N - m)/k$ . For each time interval  $k$  and the initial time  $m$  such that  $m = 1, 2, \dots, k$ , we calculate the length of  $x_m^k$  using

$$L_m^k = \frac{\sum_{i=1}^{[A]} |x_{m+ik} - x_{m+(i-1)k}|}{k} R$$

where  $R = (N - 1)/[A]k$  is the curve length normalization factor. To compute the average of curve length for each  $k$ , we calculate the mean of  $L_m^k$  for  $m = 1, 2, \dots, k$  and take the average for  $k = 1, \dots, k_{max}$ . Next, we plot  $\log(L_m^k)$  versus  $\log(1/k)$  for different time interval  $k$ . Finally, we calculate the slope of regressed line which is obtained by the least-squares approximation as the Higuchi fractal dimension for time interval  $k = 500$ . We have estimated the fractal dimension of the Arizona drought database and plotted their regression models for each data in figure (10).

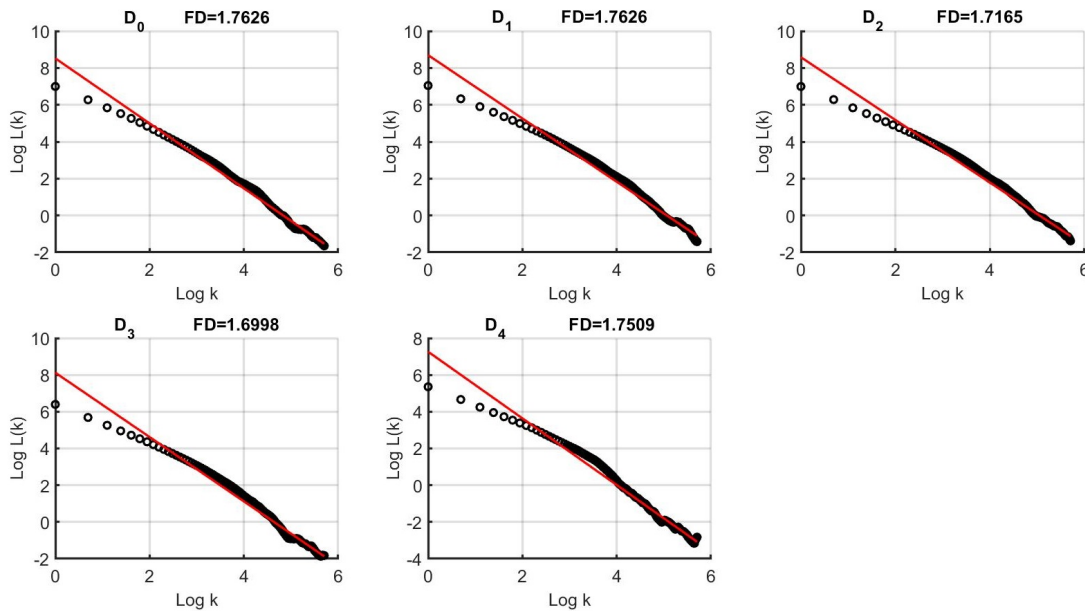


FIGURE 10. Plots of  $\log(L_m^k)$  versus  $\log(k)$  for time interval  $k = 500$ , the logarithmic scale and the corresponding slope of fitted regression line (the Higuchi fractal dimension) for Arizona Drought Monitor Categories database (2000 - present).

### 3. DISCUSSION

Drought as a slowly progressed and hidden disaster takes place in normal cycles of climate and it affects adversely environment and economic the same as other disasters. Therefore, characterizing the complexity of its nature will help to predict and recognize its different stages before it damages our societies. In U.S., the National Integrated Drought Information System (NIDIS) which is a multi-agency partnership, works on facilitating drought recording, predicting, risk management and planning at different national levels. Because of obvious impacts of drought on agriculture, water supply, energy production, public health, and wildlife, we decided to find analytical and computational techniques to characterize the complexity of different levels of drought from moderate drought  $D_1$  to exceptional drought  $D_4$  using the Arizona Drought Monitor databases. We applied the time-frequency analysis using Continuous Wavelet Transform (CWT) to visualize the non-linearity in the structure of five different groups of drought levels in the frequency domain of data vibration. Moreover, we carried out the vibration analysis using the power-law exponent and (PSD) to discover the power-law and self-similarity behaviors in the structure of drought database. we performed the multi-fractal analysis in studying the multi-fractal properties of our time series data. This analysis revealed the presence of a wide range of scaling exponent for  $D_0$ - $D_4$  and multi-fractal structure of the drought database. We continued our study by measuring the fractal complexity in drought time series data using Higuchi algorithm. This analysis helped to compare the self-similarity of different drought levels. Although these methods helped to characterize the complexity in the nature of our database, however it requires further studies to find an appropriate mathematical model (deterministic or stochastic) governing the complex dynamics of drought time series data.

### REFERENCES

- [1] Y. Ding, M.J. Hayes, M. Widhalm, Measuring economic impacts of drought: a review and discussion, *Disaster Prevent. Manage.* 20 (2011) 434–446. <https://doi.org/10.1108/09653561111161752>.
- [2] R.A. Lawes, R.S. Kingwell, A longitudinal examination of business performance indicators for drought-affected farms, *Agric. Syst.* 106 (2012) 94–101. <https://doi.org/10.1016/j.agsy.2011.10.006>.
- [3] M. Alston, J. Kent, Social impacts of drought: a report to NSW Agriculture, Centre for Rural Social Research, Charles Sturt University, Wagga, NSW, 2004. [https://www.csu.edu.au/\\_\\_data/assets/pdf\\_file/0008/704483/Social-Impacts-of-Drought.pdf](https://www.csu.edu.au/__data/assets/pdf_file/0008/704483/Social-Impacts-of-Drought.pdf).
- [4] L.M. Mosley, Drought impacts on the water quality of freshwater systems; review and integration, *Earth-Sci. Rev.* 140 (2015) 203–214. <https://doi.org/10.1016/j.earscirev.2014.11.010>.
- [5] D.A. Wilhite, M.D. Svoboda, M.J. Hayes, Understanding the complex impacts of drought: A key to enhancing drought mitigation and preparedness, *Water Resour. Manage.* 21 (2007) 763–774. <https://doi.org/10.1007/s11269-006-9076-5>.
- [6] M. Peña-Gallardo, S. Vicente-Serrano, F. Domínguez-Castro, S. Quiring, M. Svoboda, S. Beguería, J. Hannaford, Effectiveness of drought indices in identifying impacts on major crops across the USA, *Clim. Res.* 75 (2018) 221–240. <https://doi.org/10.3354/cr01519>.

- [7] H. Wu, D.A. Wilhite, An Operational Agricultural Drought Risk Assessment Model for Nebraska, USA, *Natural Hazards*. 33 (2004) 1–21. <https://doi.org/10.1023/b:nhaz.0000034994.44357.75>.
- [8] J. Christian-Smith, M.C. Levy, P.H. Gleick, Maladaptation to drought: a case report from California, USA, *Sustain. Sci.* 10 (2015) 491–501. <https://doi.org/10.1007/s11625-014-0269-1>.
- [9] H. Chang, M.R. Bonnette, Climate change and water-related ecosystem services: impacts of drought in California, USA, *Ecosyst. Health Sustain.* 2 (2016) e01254. <https://doi.org/10.1002/ehs2.1254>.
- [10] T. Tadesse, D.A. Wilhite, S.K. Harms, M.J. Hayes, S. Goddard, Drought monitoring using data mining techniques: A case study for Nebraska, USA, *Nat. Hazards*. 33 (2004) 137–159. <https://doi.org/10.1023/b:nhaz.0000035020.76733.0b>.
- [11] J.W. Nielsen-Gammon, The 2011 Texas drought, *Texas Water J.* 3 (2012) 59–95. <https://doi.org/10.21423/TWJ.V3I1.6463>.
- [12] J.S. Clark, E.C. Grimm, J.J. Donovan, S.C. Fritz, D.R. Engstrom, J.E. Almendinger, Drought cycles and landscape responses to past aridity on prairies of the northern great plains, USA, *Ecology*. 83 (2002) 595–601. [https://doi.org/10.1890/0012-9658\(2002\)083\[0595:dcalrt\]2.0.co;2](https://doi.org/10.1890/0012-9658(2002)083[0595:dcalrt]2.0.co;2).
- [13] I.W. Jung, H. Chang, Climate change impacts on spatial patterns in drought risk in the Willamette River Basin, Oregon, USA, *Theor. Appl. Climatol.* 108 (2011) 355–371. <https://doi.org/10.1007/s00704-011-0531-8>.
- [14] Y. Yang, M. Anderson, F. Gao, C. Hain, A. Noormets, G. Sun, R. Wynne, V. Thomas, L. Sun, Investigating impacts of drought and disturbance on evapotranspiration over a forested landscape in North Carolina, USA using high spatiotemporal resolution remotely sensed data, *Remote Sens. Environ.* 238 (2020) 111018. <https://doi.org/10.1016/j.rse.2018.12.017>.
- [15] R. Albarakat, V. Lakshmi, Comparison of normalized difference vegetation index derived from landsat, MODIS, and AVHRR for the mesopotamian marshes between 2002 and 2018, *Remote Sens.* 11 (2019) 1245. <https://doi.org/10.3390/rs11101245>.
- [16] K.I. Wheeler, M.C. Dietze, A statistical model for estimating midday NDVI from the geostationary operational environmental satellite (GOES) 16 and 17, *Remote Sens.* 11 (2019) 2507. <https://doi.org/10.3390/rs11212507>.
- [17] Y. Wang, C. Zhang, F.-R. Meng, C.P.-A. Bourque, C. Zhang, Evaluation of the suitability of six drought indices in naturally growing, transitional vegetation zones in Inner Mongolia (China), *PLoS ONE*. 15 (2020) e0233525. <https://doi.org/10.1371/journal.pone.0233525>.
- [18] M. Svoboda, D. LeComte, M. Hayes, R. Heim, K. Gleason, J. Angel, B. Rippey, R. Tinker, M. Palecki, D. Stooksbury, D. Miskus, S. Stephens, The drought monitor, *Bull. Amer. Meteor. Soc.* 83 (2002) 1181–1190. <https://doi.org/10.1175/1520-0477-83.8.1181>.
- [19] S. Mallat, *A wavelet tour of signal processing*, Elsevier, 1999. <https://www.di.ens.fr/~mallat/papiers/WaveletTourChap1-2-3.pdf>.
- [20] L. Rodríguez-Liñares, A.J. Méndez, M.J. Lado, D.N. Olivieri, X.A. Vila, I. Gómez-Conde, An open source tool for heart rate variability spectral analysis, *Computer Meth. Programs Biomed.* 103 (2011) 39–50. <https://doi.org/10.1016/j.cmpb.2010.05.012>.
- [21] H. Wendt, P. Abry, Multifractality tests using bootstrapped wavelet leaders, *IEEE Trans. Signal Process.* 55 (2007) 4811–4820. <https://doi.org/10.1109/tsp.2007.896269>.
- [22] H. Wendt, P. Abry, S. Jaffard, Bootstrap for Empirical Multifractal Analysis, *IEEE Signal Process. Mag.* 24 (2007) 38–48. <https://doi.org/10.1109/msp.2007.4286563>.
- [23] S. Jaffard, B. Lashermes, P. Abry, *Wavelet analysis and applications*, Springer, 201–246, 2006. <https://hal-ens-lyon.archives-ouvertes.fr/ensl-00195088>.
- [24] S. Jaffard, *Wavelet techniques in multifractal analysis*, Paris Univ. (France), 2004. <https://apps.dtic.mil/sti/pdfs/ADA433872.pdf>.

- [25] R.H. Riedi, Multifractal processes, Rice Univ. (Houston), 1999. <https://apps.dtic.mil/sti/pdfs/ADA531331.pdf>.
- [26] B.B. Mandelbrot, Possible refinement of the lognormal hypothesis concerning the distribution of energy dissipation in intermittent turbulence, *Statistical models and turbulence*, Springer, 333–351, 1972. [https://doi.org/10.1007/3-540-05716-1\\_20](https://doi.org/10.1007/3-540-05716-1_20).
- [27] R. Riedi, An Improved Multifractal Formalism and Self-Similar Measures, *Journal of Mathematical Analysis and Applications*. 189 (1995) 462–490. <https://doi.org/10.1006/jmaa.1995.1030>.
- [28] H.G.E. Hentschel, I. Procaccia, The infinite number of generalized dimensions of fractals and strange attractors, *Physica D: Nonlinear Phenomena*. 8 (1983) 435–444. [https://doi.org/10.1016/0167-2789\(83\)90235-x](https://doi.org/10.1016/0167-2789(83)90235-x).
- [29] T.C. Halsey, M.H. Jensen, L.P. Kadanoff, I. Procaccia, B.I. Shraiman, Fractal measures and their singularities: The characterization of strange sets, *Phys. Rev. A*. 33 (1986) 1141–1151. <https://doi.org/10.1103/physreva.33.1141>.
- [30] C. Panigrahy, A. Garcia-Pedrero, A. Seal, D. Rodríguez-Esparragón, N. Mahato, C. Gonzalo-Martín, An approximated box height for differential-box-counting method to estimate fractal dimensions of gray-scale images, *Entropy*. 19 (2017) 534. <https://doi.org/10.3390/e19100534>.
- [31] Y. Öztürk, Fractal Dimension as a Diagnostic Tool for Cardiac Diseases, *Int. J. Current Eng. Technol.* 9 (2019), 425–431. <https://doi.org/10.14741/ijcet/v.9.3.13>.
- [32] T. Higuchi, Approach to an irregular time series on the basis of the fractal theory, *Physica D: Nonlinear Phenomena*. 31 (1988) 277–283. [https://doi.org/10.1016/0167-2789\(88\)90081-4](https://doi.org/10.1016/0167-2789(88)90081-4).
- [33] R.S. Gomolka, S. Kampusch, E. Kaniusas, F. Thürk, J.C. Széles, W. Klonowski, Higuchi fractal dimension of heart rate variability during percutaneous auricular vagus nerve stimulation in healthy and diabetic subjects, *Front. Physiol.* 9 (2018) 1162. <https://doi.org/10.3389/fphys.2018.01162>.
- [34] M.J. Katz, Fractals and the analysis of waveforms, *Computers Biol. Med.* 18 (1988) 145–156. [https://doi.org/10.1016/0010-4825\(88\)90041-8](https://doi.org/10.1016/0010-4825(88)90041-8).